Experimental investigation into the flow behaviour of thin water films; effect on a cocurrent air flow of moderate to high supersonic velocities Pressure distribution at the surface of rigid wavy reference structures

D. E. WURZ (KARLSRUHE)

THE FIRST part of this paper reports on experimental investigations into the flow behaviour of thin water films and their effect on a cocurrent air flow of supersonic velocities ranging from moderate to high. In comparison with the paper [46] this work covers an extended Mach number range ($1.2 < M < 2.4$). In addition, the gas boundary layer has been studied more thoroughly. With regard to the results for the subsonic case we report on friction coefficient of wavy water films, mean film thickness, upper stability limit of the film flow (disturbance waves, droplet formation), temperature and velocity profiles of the cocurrent air flow. The second part of this paper is still in its teens. Since it is almost impossible to measure the pressure distribution at the interface of a wavy liquid film and a high velocity gas flow, we measured the pressure distribution along rigid wavy structures imitating the wave structure of the film. Wave length and amplitude are small with respect to the boundary layer thickness of the air flow. As could have been expected, the pressure distribution is qualitatively the same for subsonic and supersonic boundary edge velocities. A quantitative applicability of these results to theoretical approaches to film stability is questionable.

Pierwsza część tej pracy dotyczy badań eksperymentalnych nad zachowaniem się cienkich filmów wody i ich wpływu na towarzyszący przepływ powietrza w zakresie od prędkości umiarkowanych do naddźwiękowych. W porównaniu z pracą [46] praca niniejsza zawiera rozszerzony zakres liczb Macha od $M = 1.2$ do $M = 2.4$. Ponadto tutaj dokładniej została zbadana warstwa przyścienna gazu. Dla przypadku poddźwiękowego rozważono i szczegółowo przedyskutowano otrzymane wyrażenia na współczynniki tarcia pofalowanych filmów wody, uśrednioną grubość filmu, górną granicę stateczności przepływu filmu (fale zaburzenia, tworzenie się kropel), profile temperatury i prędkości towarzyszącego przepływu powietrza. Druga część tej pracy jest jeszcze w trakcie opracowania. Ponieważ jest prawie niemożliwością dokonanie pomiaru rozkładu ciśnienia na powierzchni oddzielającej pofalowany film cieczy i przepływ gazu z dużą prędkością, mierzyliśmy rozkład ciśnienia wzdłuż sztywnych pofalowynach konstrukcji imitujących falową strukturę filmu. Długość i amplituda fali są małe w stosunku do grubości przyściennej strumienia powietrza. Jak należało się spodziewać, rozkład ciśnienia ilościowo jest taki sam dla poddźwiękowej i naddźwiękowej krawędzi brzegowej. Jakościowe przyjęcie tych wyników do rozważań teoretycznych nad statecznością filmu budzi poważne zastrzeżenia.

Первая часть данной работы касается экспериментальных исследований поведения тонких пленок воды и их влияний на сопутствующее течение воздуха в интервале от умеренных до сверхзвуковых скоростей. По сравнению с работой [46], настоящая работа содержит расширенный интервал чисел Маха от $M = 1,2$ до $M = 2,4$. Кроме этого здесь точнее исследован пристеночный слой газа. Для дозвукового случая рассмотрены и подробно обсуждены полученные выражения для коэффициентов трения волнообразных пленок воды, усредненной толщины пленки, верхнего предела устойчивости течения пленки (волны возмущения, образование капель), профилей температуры и скорости сопутствующего течения воздуха. Вторая часть данной работы еще незакончена. Т. к. почти невозможно произвести измерения распределения давления на поверхности разделяющей волнообразную пленку жидкости и течение газа с большой скоростью, измерялось распределение давления вдоль жестких волнообразных конструкций, имитирующий волновую структуру пленки. Длина и амплитуда волны малы по отношению к толщине пристеночного слоя потока воздуха. Как следовало ожидать распределение давления количественно аналогично для дозвуковой и сверхзвуковой краевой грани. Качественное принятие этих результатов для теоретических рассуждений по устойчивости пленки возбуждает серьезные возражения.

Part I. Experimental investigations into the flow behaviour of thin water films and their effect on a cocurrent air flow of moderate to high supersonic velocities

1.1. Introduction

QUESTIONS concerning liquid film flow arise in many fields of technology, such as, for example, in connection with erosion damage in steam turbines [12, 16, 34], in the cooling of rocket nozzles [13, 20, 21, 22, 36] or in ablation cooling processes of re-entry vehicles [28, 37, 41] — just to mention a few high velocity applications.

1.2. Aim and scope of this investigation

Starting from subsonic gas phase velocities [44, 45] we extended our experimental work on the flow behaviour of water films into the field of moderate to high supersonic velocities. In comparison with the results for the subsonic case we report on friction coefficients of wavy water films, mean film thickness, upper stability limit of the film flow (disturbance waves, droplet formation), total temperature and velocity profiles in the cocurrent air flow.

The range of this investigation is characterized by:

Mach number of the gas flow: 1.25–2.4,
mean interfacial shear stress: 150–230 Nm^{-2},
liquid film flow rate: 0.2–0.53 $cm^3 s^{-1}\ cm^{-1}$,
mean film thickness: 20–$40 \cdot 10^{-6}$ m.

1.3. Test apparatus (Fig. 1)

The film test section is a horizontal, rectangular channel, 724 mm long and 60 mm wide. After an entrance length of 170 mm a uniform liquid film is produced on the base plate by means of a continuously adjustable slot. After a path length of 528 mm the film is completely sucked away by the aid of fine mesh screens, imbedded in the base plate. Using a mass balance it can be established whether the liquid flow in the film has decreased as a result of evaporation or droplet formation. The film base plate can be heated from below in order to produce almost constant film temperatures over the length and width of the test section.

Laval nozzle configurations are created by meas of adequately profiled plexiglass ceilings. Figure 2 gives an impression of the gas-flow conditions for a hydraulically-smooth and adiabatic base plate without a liquid film.

In nozzle I the film slot lies 35 mm in front of the critical cross section. The Mach number increases from 1.22 (plane 1) to 1.54 (plane 5), displacement and momentum thickness from 0.49 to 0.92 and 0.23 to 0.4, respectively. The wall shear stress (without film) decreases from 182 to 134 Nm^{-2}.

In nozzle III the film slot lies 126 mm downstream of the critical cross section. The Mach number is almost constant, the shear stress decreases and differs only by a small amount
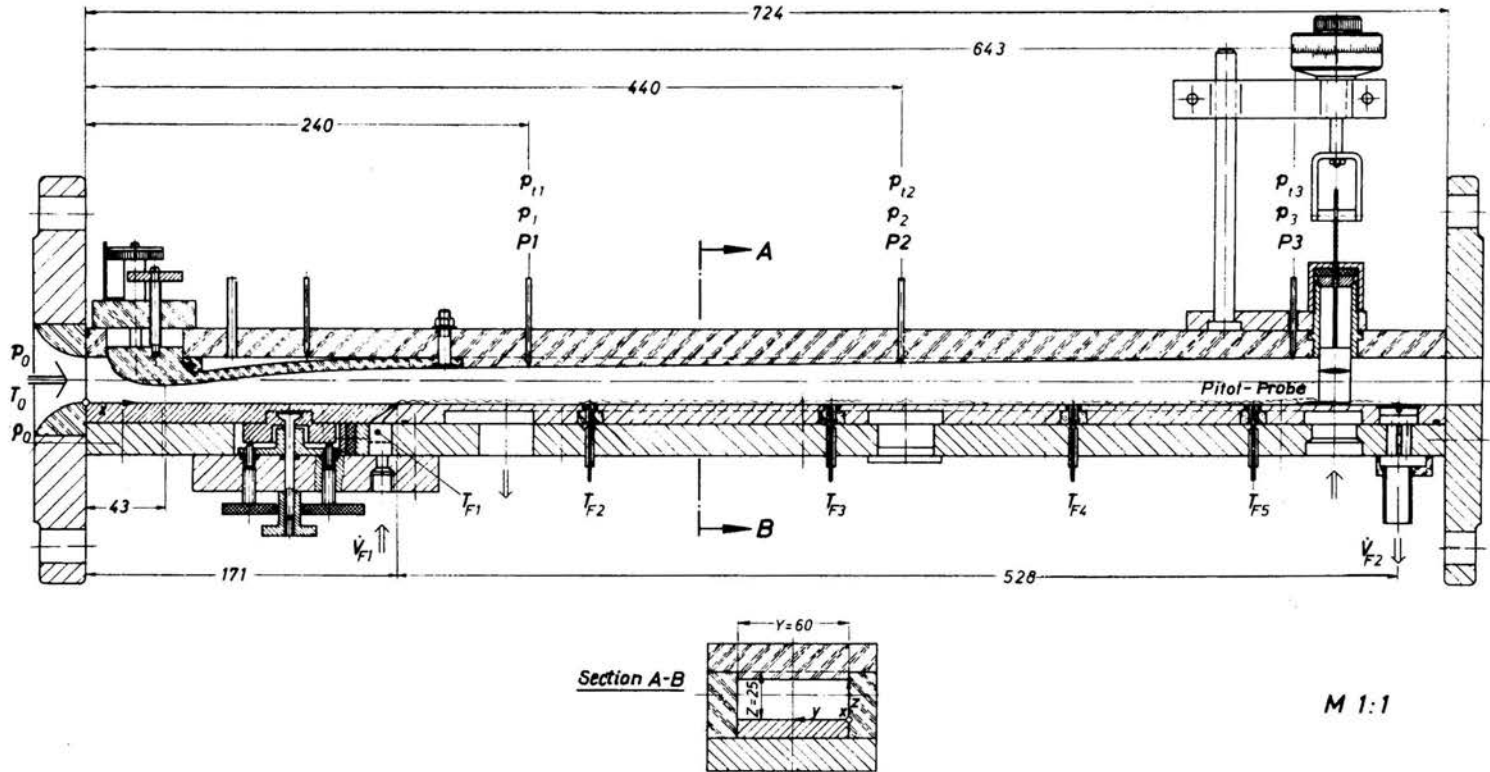
FIG. 1. Test section.
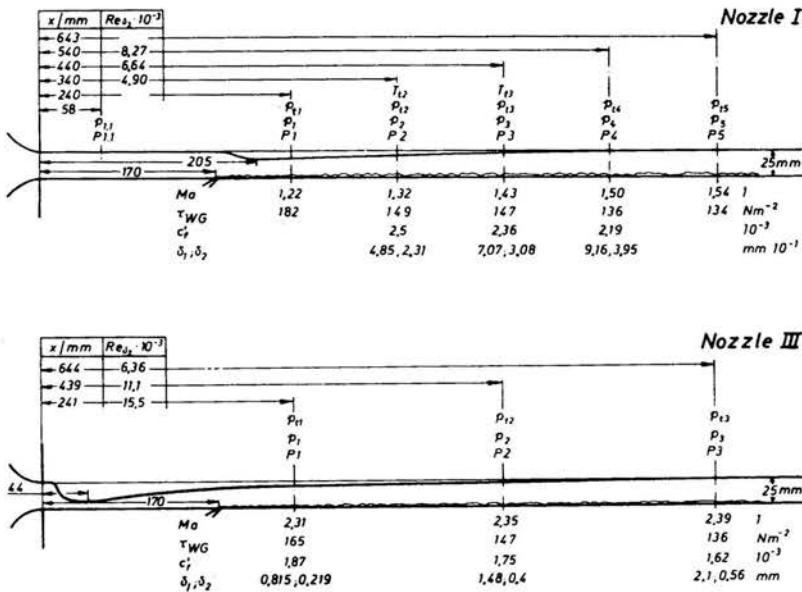
Fig. 2. Laval-nozzles I and III.

from the conditions in nozzle I. The displacement thickness increases from 0.82 to 2.1 mm, the momentum thickness from 0.22 to 0.56 mm.

1.4. Measured quantities (Fig. 1)

Stagnation values of the air flow: p_0, T_0, φ_0,
liquid film flow rate at the entrance: $\dot{V}_{F1}$ and at the outlet: $\dot{V}_{F2}$,
liquid film temeratures: T_{F1}, ..., T_{F5},
total temperature profiles in plane 2 and 3, of nozzle I: $T_t(z)$,
the total temperature probe has been built following the principles of MEIER [27];
Mach number profiles in three measuring planes using a Pitot-probe;
the outer diameter of the Pitot-probe is 0.42 mm, the inner diameter 0.2 mm.

The shaft of the Pitot-probe is a slender profile thus reducing the disturbance of the gas boundary layer, Fig. 1. The corresponding static pressure holes have a diameter of 0.4 mm.

1.5. Evaluation

1.5.1. Wall shear stress. The wall shear stress τ_{WG} for dry wall conditions is evaluated following the Preston method (Fig. 3) from the readings gained via a Pitot-probe leaning against the wall. We used a calibration formula for supersonic flows, as proposed by ALLEN [2]:

(1.1) $$\log_{10} F_2 = 0.01659 \log_{10}^2 F_1 + 0.7665 \log_{10} F_1 - 0.4681,$$

(1.2) $$F_1 = \frac{\varrho'}{\varrho_\delta} \frac{\eta_\delta}{\eta'} R_D \frac{c}{c_\delta},$$

(1.3) $$F_2 = \sqrt{\frac{\varrho'}{\varrho_\delta} \frac{\eta_\delta}{\eta'} R_D \sqrt{c'_{fWG}}},$$

$$F_1 = \frac{\varrho'}{\varrho_\delta}\frac{\eta_\delta}{\eta'}R_D\frac{c}{c_\delta}$$

$$F_2 = \sqrt{\frac{\varrho'}{\varrho_\delta}}\frac{\eta_\delta}{\eta'}R_D\sqrt{c'_{iWG}}$$

$$R_D = \frac{\varrho_\delta c_\delta D}{\eta_\delta}\ ;\quad c'_{iWG} = \frac{\tau_{WG}}{\frac{1}{2}\varrho_\delta c_\delta^2}$$

$$T' = T_\delta(1+0.1142\,M_\delta^2)$$

$$\varrho' = \varrho(T')\ ;\quad \eta' = \eta(T')$$

J.M. Allen [2]

$$\log_{10}F_2 = 0.01659\ \log_{10}^2 F_1 + 0.7665\ \log_{10}F_1 - 0.4681$$
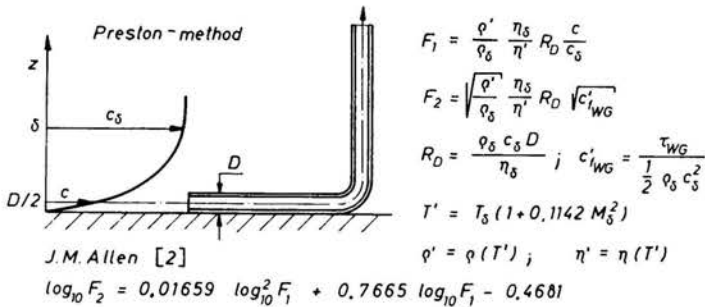
FIG. 3. Preston-method.

(1.4)
$$R_D = \frac{\varrho_\delta c_\delta D}{\eta_\delta}, \qquad c'_{fWG} = \frac{\tau_{WG}}{\frac{1}{2}\varrho_\delta c_\delta^2},$$

(1.5)
$$T' = T_\delta(1+0.1142\,M_\delta^2),$$

(1.6)
$$\varrho' = \varrho(T'), \quad \eta' = \eta(T').$$

The wall distance $D/2$ of the centre of the Pitot-probe has not been corrected with respect to wall and shear layer effects. The velocity $c_{D/2}$ has been calculated on the assumption of constant total temperature across the boundary layer.

1.5.2. Interfacial shear stress. The interfacial shear stress τ_{FG}, i.e., the mean drag acting at the wavy film-gas interface, is composed of skin friction and form drag. This essential parameter was determined in two different ways.

a) In accordance with ELLIS and GAY [10] the shear stress at the interface of a liquid film and a propelling gas flow can be determined from the slope of a semilogarithmic plot of the measured air velocity profiles (Fig. 4). In this case the following equation holds:

(1.7)
$$\tau_{FG} = \varrho_W\left[\varkappa'\frac{c_2-c_1}{\ln(z_{2k}/z_{1k})}\right]^2,$$

$\varkappa'$ is the von Kármán constant. We chose a value of $\varkappa' = 0.4$, resulting in the smallest over-all deviation from those results which were determined using the boundary layer momentum equation. c_1 and c_2 are two velocities out of the linear range of the non-dimensional velocity profile, z_{1k} and z_{2k} are the corresponding corrected wall distances.

In order to obtain better accuracy in evaluating the interfacial shear stress, the wall distance must be corrected by taking into account the film thickness as well as wall and shear layer effects. This must be done by an iterative procedure since the shear stress itself must be known for these corrections. As a first correction step the zero mark of the wall distance is placed on the plane of the mean film thickness. In a second correction step wall and shear layer effects are considered.

In nozzle I the velocities c_1 and c_2 in Eq. (1.7) are always subsonic, and there is no reason why we should not correct the wall distance using the results for subsonic boundary layers [25]. In nozzle III the velocities c_1 and c_2 are always supersonic. Here the situation is complicated by the fact that the results of the potential investigations are contradictory

17*
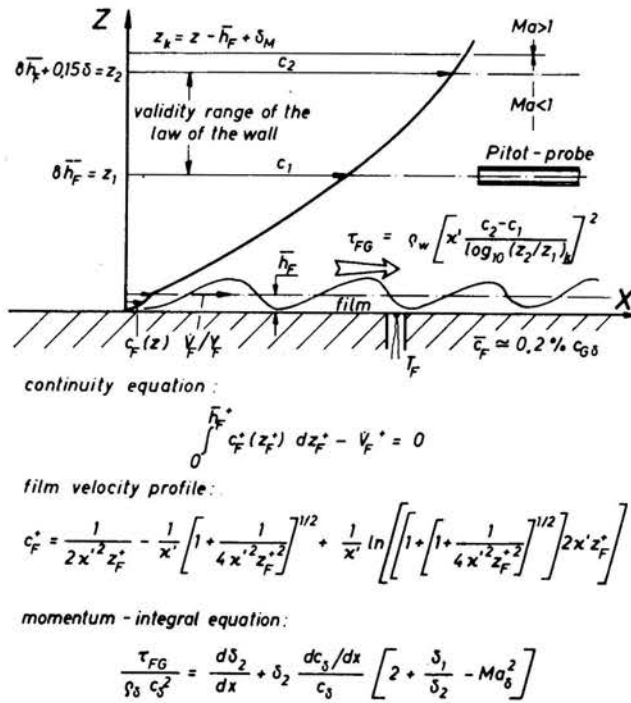
FIG. 4. Evaluation of interfacial shear stress and mean film thickness.

[1, 7, 43]. MEIER [26] found that the deviation of measured supersonic velocity profiles from theoretical values (law of the wall for compressible boundary layers) is reduced by a positive correction, shifting the measured profiles towards larger wall distances, by an amount which differs scarcely from the corrections proposed by McMillan for incompressible boundary layers. For this reason we applied the McMillan corrections to each of the measured velocity profiles.

The combination of the two corrections with respect to film thickness and wall and shear layer effects produces the corrected wall distance:

$$(1.8) \qquad z_k = z + \delta_M - \bar{h}_F.$$

b) As a result of a more thorough investigation of the air boundary layer it is possible to calculate the interfacial shear stress from the momentum-integral equation for two-dimensional compressible boundary layers:

$$(1.9) \qquad \frac{\tau_{FG}}{\varrho_\delta c_\delta^2} = \frac{d\delta_2}{dx} + \delta_2 \frac{dc_\delta/dx}{c_\delta} \left[2 + \frac{\delta_1}{\delta_2} - Ma_\delta^2 \right],$$

$$(1.10) \qquad \delta_1 = \int_0^\delta \left(1 - \frac{\varrho c}{\varrho_\delta c_\delta} \right) dy,$$

$$(1.11) \qquad \delta_2 = \int_0^\delta \frac{\varrho c}{\varrho_\delta c_\delta} \left(1 - \frac{c}{c_\delta} \right) dy.$$

1.5.3 Mean film thickness (Fig. 4). The mean film thickness could be measured "directly" [6]. But it is known that — starting from liquid state, liquid flow rate and interfacial shear — a mean film thickness can be calculated with sufficient accuracy [8, 9, 45].

We calculate the mean film thickness $\bar{h}_F$ from the upper integration limit of the continuity equation (1.12), using a film velocity profile $c_F(z)$ (1.13), which was deduced some years ago [45]

$$\text{(1.12)} \qquad \int_0^{\bar{h}_F^+} c_F^+(z_F^+)\,dz_F^+ - \dot{V}_F^+ = 0,$$

$$\text{(1.13)} \qquad c_F^+ = \frac{1}{2\varkappa'^2 z_F^+} - \frac{1}{\varkappa'}\left\{1 + \frac{1}{4\varkappa'^2 z_F^{+2}}\right\}^{1/2} + \frac{1}{\varkappa'}\ln[[1 + \{1 + 1/(4\varkappa'^2 z_F^{+2})\}^{1/2}]2\varkappa' z_F^+].$$

1.6. Results

1.6.1. Friction coefficient for dry wall conditions. Figure 5 shows a plot of the local friction coefficient — determined according to the Preston method — versus the gas Reynolds number $Re_{\delta 2}$ based on the momentum thickness δ_2. The results coincide with the
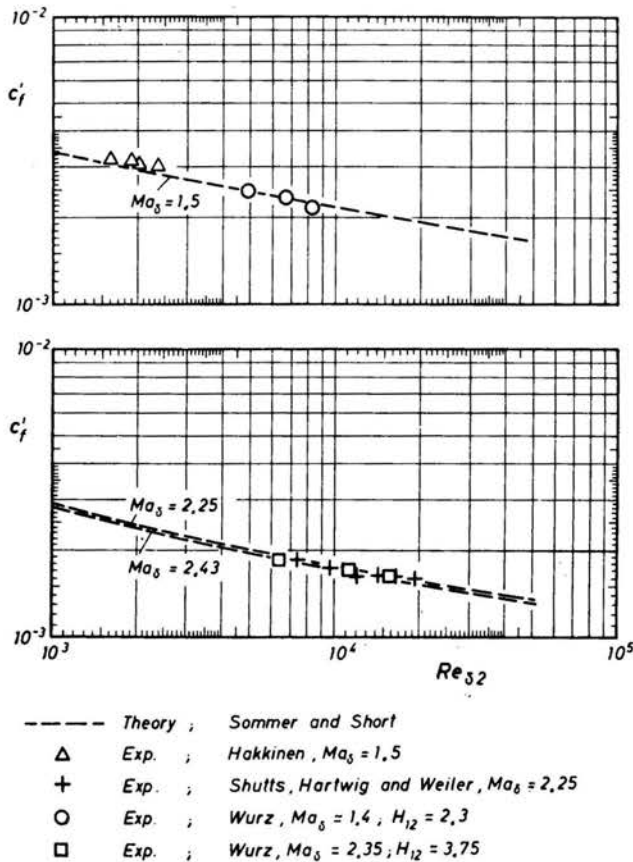
FIG. 5. Friction coefficients for dry wall conditions.

SOMMER and SHORT theory [40] and with the experimental results of HAKKINEN [17] and SHUTTS [39], respectively.

1.6.2 Interfacial shear stress and upper stability limit. Figures 6 and 7 show the dependence of the interfacial shear stress on the specific liquid flow rate for nozzle I and nozzle II. The blank marks indicate the results which have been determined from the slope of the air velocity profiles (1.7) and the fat marks indicate the results from the momentum-integral equation (1.9). The deviation from mean curves is below 9% and 6% for low and high Mach number conditions, respectively. In both cases the liquid film increases the shear stress by approx. 30% in comparison with the dry wall condition ($\dot{V}_F/Y_F = 0$).
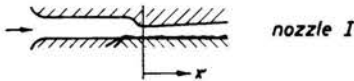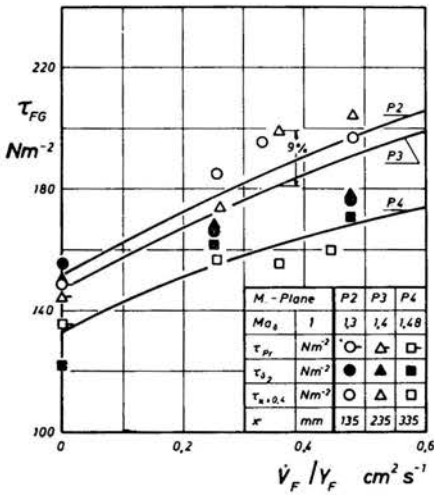
FIG. 6. Interfacial shear stress.
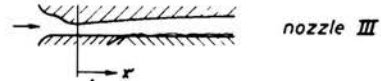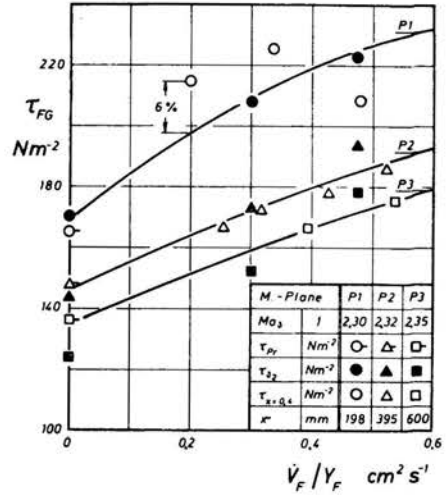
FIG. 7. Interfacial shear stress.
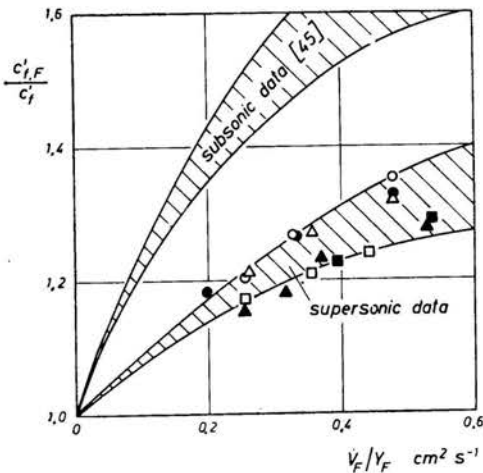
FIG. 8. Friction coefficients of wavy water films.

The upper limit of the stable film flow range is reached for liquid flow rates of about 0.45–0.5 $cm^3 s^{-1}$. Under high shear conditions this critical flow rate is almost independent of the interfacial shear stress [20, 45, 46].

1.6.3 Friction coefficient of wavy water films (Fig. 8). For supersonic gas flow velocities the relation of the interfacial shear stress to the dry wall shear stress $c'_{f,F}/c'_f$ increases less steeply as, compared with the subsonic results. A corresponding tendency has been found by GODDARD [15] for sand-roughened walls.

1.6.4 Mean film thickness. Figure 9 shows a plot of the calculated mean film thickness against liquid flow rate. Accordingly, the mean thickness of the stable film was between 20 and 40 μm. For specific water flow rates below 0.2 $cm^3 s^{-1} cm^{-1}$ the film tends to split into rivulets.
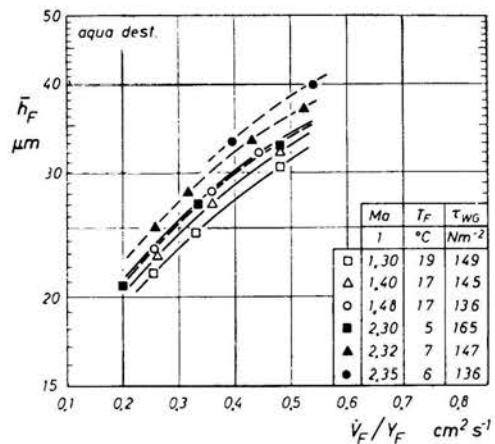
FIG. 9. Mean film thickness.

1.6.5. Total temperature profiles. Figure 10 shows an example of the measured total temperature profiles. In order to avoid condensation effects the air has been dried. This results in psychrometric effects reducing the film temperature. To prevent icing the liquid film must be heated from below, producing diabatic wall conditions. These total temperature profiles resemble quite closely those measured by MEIER [49] in the case of diabatic one-phase flows.

For reasons of a compressor damage the total temperature profiles have not yet been measured under high Mach number conditions. The corresponding velocity profiles have been calculated on the base of linear total temperature profiles connecting the measured wall and boundary edge temperatures:

$$(1.14) \qquad \frac{T_t}{T_{t\delta}} = (1 - T_F/T_{t\delta})\mathsf{M}(z)/\mathsf{M}_\delta + T_G/T_{t\delta}.$$

In the low Mach number nozzle, these linear profiles differ from the measured profiles by a figure of less than 1% (Fig. 10). The resulting error in the velocities is below 0.5%, which is almost insignificant as compared to the uncertainties in the effective wall distances of the Pitot-probe. Under high Mach number conditions the errors should be of the same order of magnitude.
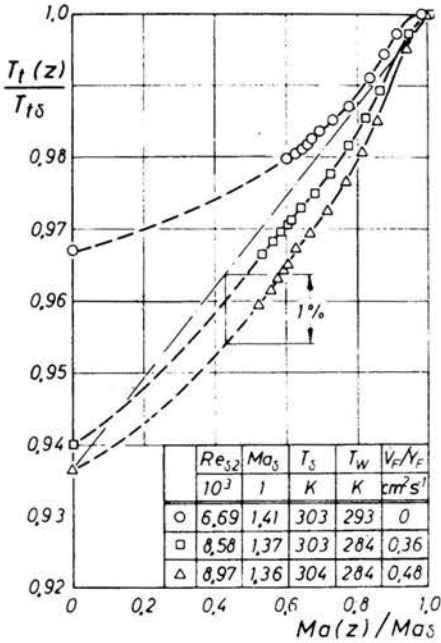
FIG. 10. Total temperature profiles.

1.6.6. Non-dimensional velocity profiles. Figures 11 and 12 show typical air velocity profiles in the usual non-dimensional form. The profiles for dry and smooth wall conditions follow quite closely the straight line characterized by a roughness Reynolds number of $Re_s = 5$. The liquid films cause a velocity defect, shifting the velocity profiles towards higher roughness Reynolds numbers. A comparison of the equivalent sand roughness — computed from Re_s — with the mean film thickness results in a ratio of about 1.5 (last two columns of Tables 1 and 2).

Table 1. Data relating to Fig. 11

$\dot{V}_F/Y_F$ cm²s⁻¹	M_δ 1	$\sqrt{\tau_w/\varrho_w}$ ms⁻¹	δ mm	δ_1 mm	δ_2 mm	H_{12} 1	$\bar{h}_F$ 10⁻³mm	k_S 10⁻³mm
0	1.41	16.4	3.6	0.707	0.308	2.30	0	0
0.26	1.37	17.7	4.1	0.844	0.369	2.29	23	33
0.36	1.37	17.9	4.2	0.887	0.393	2.26	27	41
0.48	1.36	18.1	4.3	0.925	0.410	2.26	32	48

Table 2. Data relating to Fig. 12

$\dot{V}_F/Y_F$ cm²s⁻¹	M_δ 1	$\sqrt{\tau_w/\varrho_w}$ ms⁻¹	δ mm	δ_1 mm	δ_2 mm	H_{12} 1	$\bar{h}_F$ 10⁻³mm	k_S 10⁻³mm
0	2.37	23.1	7.8	2.11	0.557	3.78	0	0
0.39	2.24	23.6	8.6	2.48	0.682	3.63	33	54
0.54	2.22	23.8	8.73	2.53	0.724	3.51	40	66
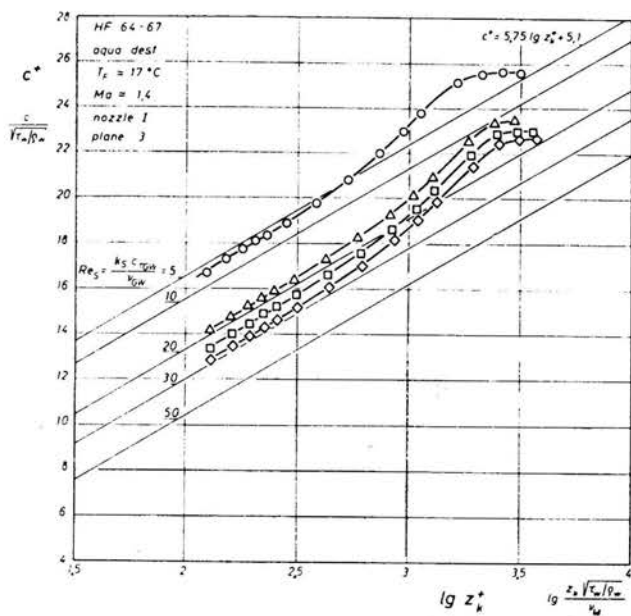
FIG. 11. Non-dimensional air velocity profiles (Data: Table 1).
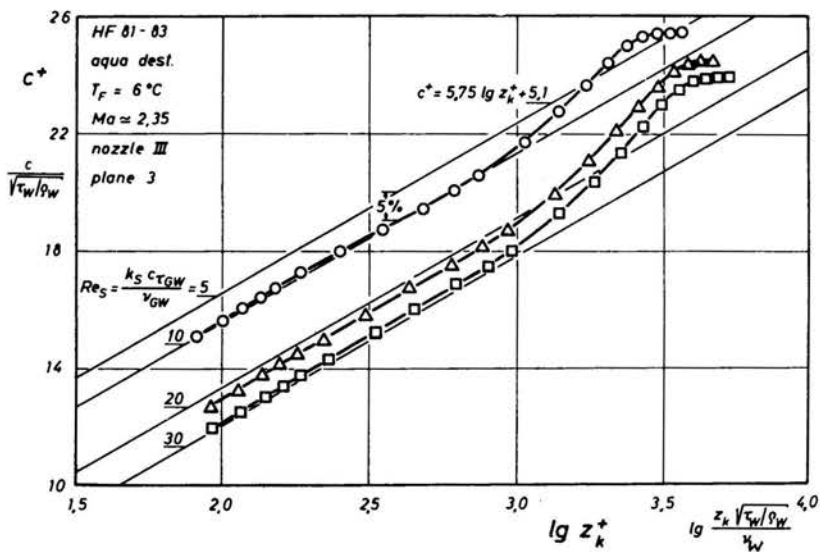
FIG. 12. Non-dimensional air velocity profiles (Data: Table 2).

[979]
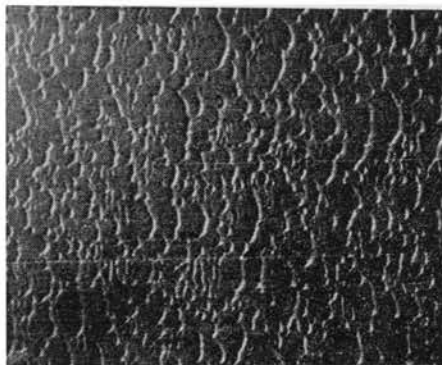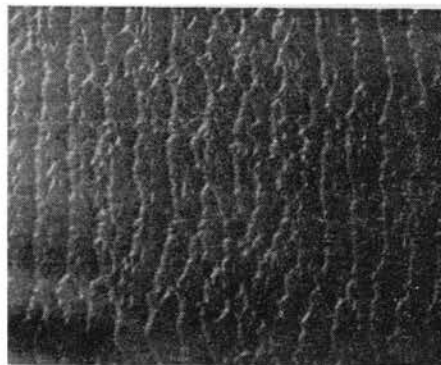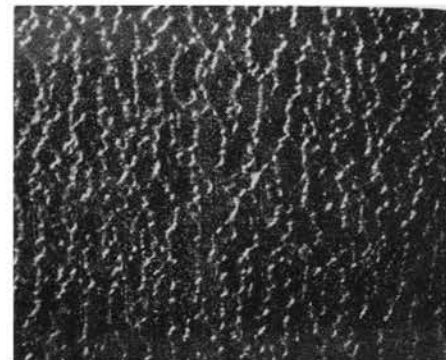
FIG. 13. Water films under the effect of a subsonic air flow (Data: Table 3).

5 mm
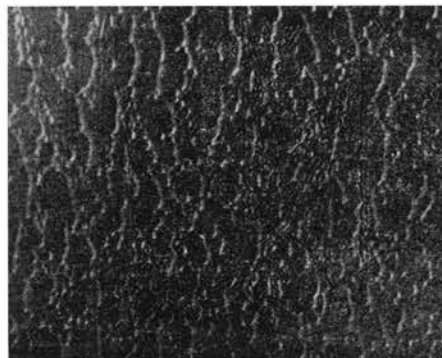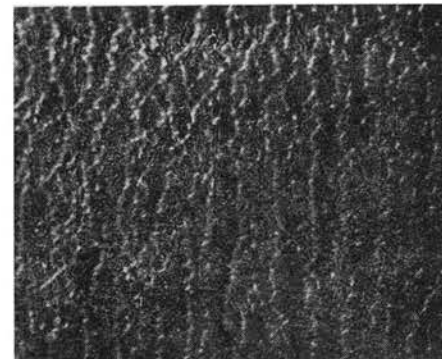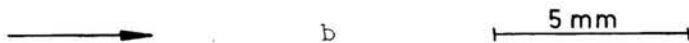
FIG. 14. Water films under the effect of a supersonic air flow (Data: Table 4).

1.6.7. Wave structure of water films (Figs. 13 and 14, Tables 3 and 4). The results concerning the wave structure of water films have not yet been evaluated systematically. Figures 13 and 14 show a comparison of photo-series of liquid films exposed to subsonic and supersonic air flows. Liquid flow rate and interfacial shear are almost the same. If there is a change at all in surface structure, switching from subsonic to supersonic velocities, then it is weak and not characteristic. In the supersonic case the wave structure seems to be a little bit more two-dimensional for low liquid flow rates, Figs. 13b and 14b. Furthermore, the mean wavelength is slightly increased by a supersonic gas flow.

Table 3. Data relating to Figs. 13a-c.
Water films under the effect of a subsonic air flow.

Fig. 13 —	M 1	$\dot{V}_F/Y_F$ cm^2/s	τ_{FG} N/m^2	$\bar{h}_F$ μm
a	0.77	0.06	150	12
b	0.78	0.22	187	23
c	0.79	0.35	200	31

Table 4. Data relating to Figs. 14a-c.
Water films under the effect of a supersonic air flow.

Fig. 14 —	M 1	$\dot{V}_F/Y_F$ cm^2/s	τ_{FG} N/m^2	$\bar{h}_F$ μm
a	1.3	0.11	158	16
b	1.29	0.204	167	21
c	1.28	0.36	180	27

Résumé of Part 1

The roughness effect of wavy water films on a cocurrent air flow can be compared with the effect of sand-roughened walls. Psychrometric effects cause a change of the total temperature profiles across the air boundary layer. Upper and lower stability limits of water films depend mainly on the interfacial shear stress. Switching from subsonic to supersonic Mach numbers will cause no characteristic change in the wave structure and the stability of water films if the boundary layer is thick enough. We need much more experimental results to clarify the influence of path length, liquid and gas properties on gas-liquid film-flows.

Part 2. Pressure distribution at the surface of rigid wavy reference structures

2.1. Introduction

Theoretical approaches to the kind of gas-liquid film-flow as studied here are extremely difficult, the gas flow being viscid, turbulent, compressible and interacting with a travelling wavy surface which is continuously adjusting its geometry to inner and outer force fields.

The occurrance of flow separation somewhere behind the wave crests — which is most likely in high velocity gas-water film-flows — introduces an additional complication. The position of separation and reattachment points depends on the turbulence which is changed in the region close to the wall by "roughness effects" of the disturbed interface. The approaches of theoretical investigations to this complex phenomenon are not sufficiently close. Most of them are restricted to sine wave geometries with relatively small amplitudes, thus preventing flow separation — to mention only one critical points. Nevertheless, some of these investigations provide valuable qualitative information on the influence of gas mean velocity profiles, as well as of compressibility on film stability, and some other interesting features [47], [48].

2.2. Aim and scope of this investigation

In order to gain a better knowledge of the pressure distribution on rigid waves imitating the interfacial structure of gas-water film-flows we started an experimental investigation which is still in its teens. This premature publication can be justified by the purpose of preventing others from investing too much into theoretical approaches to film stability, starting from imaginary models.

2.3. Test apparatus and results

The base plate of the film-test-section described in Sect. 1.3 was replaced by wavy wall elements (Figs. 15 and 16).

In a first step we studied the pressure distribution developing at the surface of 4 rotatable cylinders imbedded in a plane, hydraulically-smooth wall exposed to a flow with boundary edge Mach numbers ranging from 0.57 to 2.33, Fig. 15. The protrusion of the cylinders
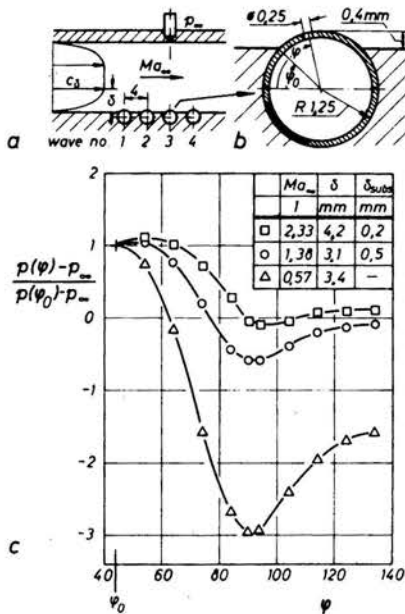
FIG. 15. Pressure distribution at the surface of imbedded cylinders.
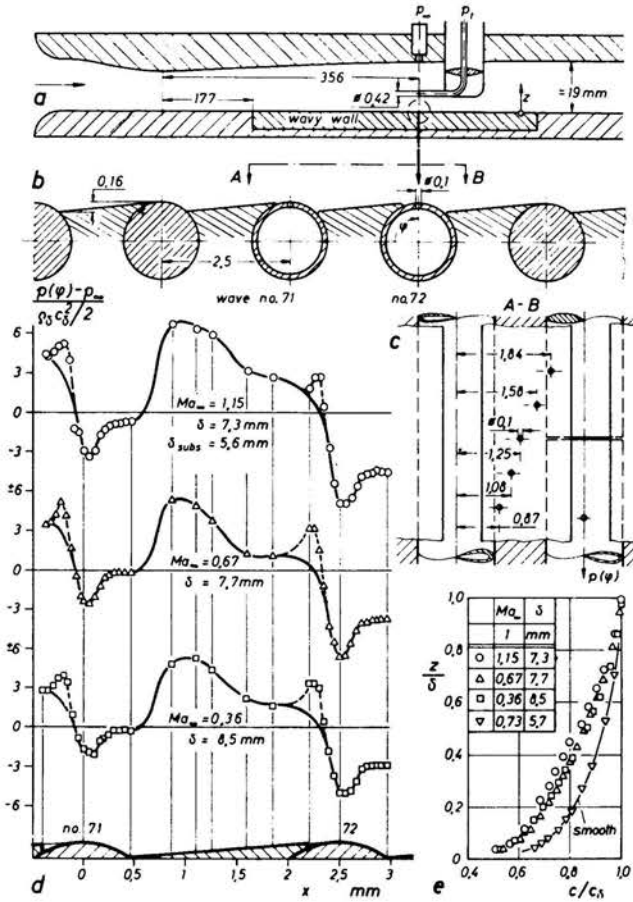
FIG. 16. Pressure distribution at the surface of a multi-wave element, and air velocity profiles.

into the gas flow is 0.4 mm, which is about 1/10th of the boundary layer thickness. The diameter of the static pressure hole is 0.25 mm, averaging over an angular range of 15°.

Figure 15c shows the results for wave no. 3. A low qualitative difference between the pressure distribution for subsonic and supersonic edge Mach numbers develops in the upstream region of the wave back. In the vicinity of the wave crest and in its downstream portion the character of the pressure distribution is almost the same.

Low viscosity liquid films, such as water films, have much lower wave amplitudes under high shear conditions (see Sect. 1.6.6). There will be no direct interaction with a moderately supersonic external flow after a short path length, and switching from subsonic to supersonic boundary edge velocities will not produce a noticeable change in the stability characteristics of water films.

In a second step we studied the pressure distribution at wave no. 71 and 72 of a multi-wave element, Fig. 16. Additionally, we measured velocity profiles in the gas boundary layer.

In this case the wave geometry, composed of a sloped back and a rotatable imbedded hypodermic needle, is supposed to be much closer to the actual interfacial geometry of a gas-water film-flow (for comparison see Fig. 14b). The diameter of the pressure holes — five holes on the back, one hole on the needle — is 0.1 mm. The exactness of these tiny wavelets is not yet completely satisfactory, above all the transition from the wave back to the needle is not smooth enough what results in a "local" pressure rise upstream of the wave crests (dotted line in Fig. 16d). Further downstreams the pressure first decreases and then increases quite similarly to the pressure at the surface of a free cylinder. Flow separation occurs at an angle of about 110°. A region of constant pressure is followed by a second pressure rise up to a stagnation point on the wave back. From this point the pressure falls towards the following wave crest. A local pressure rise is again caused by deviations from the ideal geometry.

The wavy wall produces a roughness effect on the gas boundary layer and, consequently, a deviation from the velocity profile for smooth wall conditions (Fig. 16e).

Résumé of Part 2

A subsonic wall pressure distribution exists in the presence of a supersonic external flow if the boundary layer thickness is comparable to the wave length. This confirms an essential result of INGER's and WILLIAMS's [48] investigation on subsonic and supersonic flows past low amplitude sine waves. Rigid wave geometries, which are supposed to imitate quite closely the interfacial geometry of gas-water film-flows, cause flow separation. With respect to the flow past a free cylinder the separation point is shifted downstream, presumably as the cumulated effect of a faintly sloped wave back and of the increased turbulence in the region close to the wall.

These initial results are not completely satisfactory; the investigation will be continued in order to clarify the influence of flow path length and wave geometry on wall pressure distributions.

Symbols

$a = \sqrt{\varkappa R T}$ (m s^{-1}) velocity of sound,

c (m s^{-1}) flow velocity in x-direction

c_F (m s^{-1}) flow velocity of the film,

$c_\tau = \sqrt{\tau_w/\varrho_w}$ (m s^{-1}) shear velocity,

$c^+ = c/c_\tau$ (1) dimensionless velocity,

$\bar{c}_F$ (m s^{-1}) mean flow velocity of the film,

$c'_f = 2\tau/(\varrho_\delta c_\delta^2)$ (1) local skin friction coefficient,

$c_F^+ = c_F/\sqrt{\bar{\tau}_{FG}/\varrho_F}$ (1) dimensionless flow velocity of the film,

c_δ (m s^{-1}) flow velocity at boundary layer edge,

D (m) outer diameter of Pitot or Preston tube,

$P1; P2...$ measuring planes (Figs. 1 and 2),

$F1; F2$ (1) abbreviations, Eq. (1.2) and (1.3),

$\bar{h}_F$ (m) mean film thickness,

$\bar{h}_F^+ = \bar{h}_F \sqrt{\bar{\tau}_{FG}/\varrho_F}/\nu_F$ (1) dimensionless mean film thickness,

$k_S = \mathrm{Re}_S \nu_w/c_\tau$ (m) equivalent sand roughness,

$M = c/a$ (1) Mach number,

p (N m^{-2}) pressure, static,

Re	(1)	Reynolds number,
$\mathrm{Re}_S = k_S c_\tau / \nu_W$	(1)	roughness-Reynolds number,
$\mathrm{Re}_{\delta 2} = \dfrac{c_\delta \cdot \delta_2}{\nu_\delta}$	(1)	Reynolds number based on momentum thickness,
T	(K)	temperature,
$T_{F1} \ldots T_{F5}$	(K)	film temperatures (Fig. 1),
T'	(K)	reference temperature,
$\dot{V}_F$	(cm³ s⁻¹)	liquid volume flow,
$\dot{V}_F^+ = \dot{V}_F / (\nu_F Y_F)$	(1)	dimensionless film liquid flow,
$\dot{V}_{Fkr}$	(cm³ s⁻¹)	critical liquid volume flow, beginning of droplet formation,
x, y, z	(m)	coordinates (Fig. 1),
Y_F	(m)	width of liquid film,
z_k	(m)	corrected distance from the wall Eq. (1.8),
$z_k^+ = z_k c_\tau / \nu_W$	(1)	dimensionless corrected wall distance,
$z_F^+ = z \sqrt{\overline{\tau_{FG}/\varrho_F}} / \nu_F$	(1)	dimensionless wall distance in liquid film,
δ	(m)	boundary layer thickness for $c_\delta = 0.99\, c_{max}$,
δ_1	(m)	displacement thickness (1.10),
δ_2	(m)	momentum thickness (1.11),
δ_M	(m)	correction of wall distance (1.8),
η	(kg m⁻¹ s⁻¹)	dynamic viscosity,
η'	(kg m⁻¹ s⁻¹)	reference viscosity $(1.6)_2$,
$\varkappa'$	(1)	mixing length constant,
$\varkappa$	(1)	ratio of specific heats,
$\bar{\lambda}_h$	(m)	mean wave length,
ν	(m² s⁻¹)	kinematic viscosity,
ϱ	(kg m⁻³)	density,
ϱ'	(kg m⁻³)	reference density $(1.6)_1$,
τ	(N m⁻²)	shear stress,
ϕ	(rad)	angular position (Fig. 15).

Indices

f	friction,
F	liquid,
FG	between liquid film and air,
G	air,
k	corrected,
kr	critical,
t	total,
W	wall,
WF	between rigid wall and liquid,
WG	between rigid wall and air,
δ	boundary layer edge,
o	stagnation value,
∞	outside of boundary layer.

References

1. J. M. ALLEN, *Pitot-probe displacement in a supersonic turbulent boundary layer*, NASA TN D-6759, 1972.
2. J. M. ALLEN, *Evaluation of compressible-flow Preston tube calibrations*, NASA TN D-7190, 1973.

3. I. D. CHANG and P. E. RUSSEL, *Stability of a liquid layer adjacent to a high-speed gas stream*, The Physics of Fluids, 8, 1018–1026, 1965.
4. S. F. CHIEN, and W. E. IBELE, *A literature survey. The hydrodynamic stability of the liquid film in falling film flow and in vertical annular, two-phase flow*, Int. J. Mech. Sci., 9, 547–557, 1967.
5. L. S. COHEN and T. J. HANRATTY, *Effect of waves at a gas-liquid interface on a turbulent air stream*, J. Fl. Mech., 31, 467–479, 1968.
6. J. G. COLLIER and G. F. HEWITT, *Film thickness measurement in two-phase flow*, Brit. Chem. Eng., 12, 709–715, 1967.
7. F. V. DAVIES, *Some effects of Pitot size on the measurement of boundary layers in supersonic flow*, Royal Aircraft Est. TN AERO 2179, 1959.
8. A. E. DUKLER and O. P. BERGELIN, *Characteristics of flow in falling liquid films*, Chem. Eng. Progr., 48, 557–563, 1952.
9. A. E. DUKLER, *Fluid mechanics and heat transfer in vertical falling film systems*, Chem. Eng. Progr. Symp., Ser. 56, 30, 1960.
10. S. R. M. ELLIS and B. GAY, *The parallel flow of two fluid streams. Interfacial shear and fluid-fluid interactions*, Trans. Inst. Chem. Eng., 37, 206–213, 1959.
11. G. D. FULFORD, *The flow of liquids in thin films*, Chap. 4 in Advances in Chemical Engineering, 5, 151–236, 1964.
12. G. C. GARDNER, *Some aspects of the flow of liquids as films and drops*, Report RD(P)M10, Central Electricity Generating Board, England.
13. R. A. GATER, *A fundamental investigation of the phenomena that characterize liquid-film cooling*, Purdue Univ., Lafayette, Indiana Rep. No. TM-69-1, NASA CR-105904, 1969.
14. R. A. GATER, *Correlation of liquid-film cooling mass transfer data*, Int. J. Heat Mass Trans., 15, 1956–1960, 1972.
15. F. E. GODDARD jr., *Effect of uniformly distributed roughness on turbulent skin-friction drag at supersonic speeds*, J. Aero/Space Sc., 26, 1, 1–15, 1959.
16. G. GYARMATHY, *Grundlagen einer Theorie der Nassdampfturbine*, Diss. ETH, Zurich 1960.
17. R. J. HAKKINEN, *Measurements of turbulent skin friction on a flat plate at transonic speeds*, NACA TN-3486, 1955.
18. T. J. HANRATTY and D. E. WOODMANSEE, *Stability of the interface for a horizontal air-liquid flow*, Proc. Symp. on Two-Phase Flow, Exeter 21–23 June, 1965.
19. E. J. HOPKINS and E. R. KEENER, *Study of surface Pitots for measuring turbulent skin friction at supersonic Mach numbers — adiabatic wall*, NASA TN D-3478, 1966.
20. G. R. KINNEY, A. E. ABRAMSON and J. L. SLOOP, *Internal-liquid-film-cooling experiments with airstream temperatures to 2000-F in 2-and 4-inch-diameter horizontal tubes*, NACA Rep. 1087, 1952.
21. E. L. KNUTH, *The mechanics of film cooling. Part 1*, Jet Prop., 24, 359–365, 1954.
22. E. L. KNUTH, *The mechanics of film cooling. Part 2*, Jet Prop., 25, 16–25, 1955.
23. St. C. LUBARD and J. A. SCHETZ, *Atomization and vaporization of a liquid sheet exposed to a supersonic airstream*, AIAA Paper No. 68-643, 1968.
24. B. W. MARSHALL, *An experimental investigation of a liquid film on a horizontal flat plate in a supersonic gas stream*, Oklahoma State Univ., Thesis, May 1971.
25. F. A. MCMILLAN, *Experiments on Pitot-tubes in shear flow*, ARC R. and M., 3028, 1956.
26. H. U. MEIER, *Messungen von turbulenten Grenzschichten an einer wärmeisolierten Wand im kleinen Überschallwindkanal der AVA*, Z. Flugwiss., 17, 1, 1–8, 1969.
27. H. U. MEIER, R. E. LEE and R. L. VOISINET, *Vergleichsmessungen mit einer Danberg-Temperatursonde und einer kombinierten Druck-Temperatur-Sonde in turbulenten Grenzschichten bei Überschallströmung*, Z. Flugwiss. 22, 1, 1–9, 1974.
28. Ph. R. NACHTSHEIM and J. R. HAGEN, *Observations of cross-hatched wave patterns in liquid films*, AIAA-J., 10, 12, 1637–40, 1972.
29. A. H. NAYFEH and W. S. SARIC, *Non-linear Kelvin-Helmholtz instability*, J. Fl. Mech., 46, 2, 209–31, 1971.
30. A. H. NAYFEH and W. S. SARIC, *Stability of a liquid film*, AIAA- J., 9, 4, 750–52, 1971.

31. A. H. NAYFEH and W. S. SARIC, *Non-linear waves in a Kelvin-Helmholtz flow*, J. Fl. Mech., **55**, 2, 311–27, 1972.
32. A. H. NAYFEH and W. S. SARIC, *Non-linear stability of a liquid film adjacent to a supersonic stream*, J. Fl. Mech., **58**, 1, 39–51, 1973.
33. R. F. PROBSTEIN, *Cross-hatching. A material response phenomena*, AIAA-J., 8, 364–66, 1970.
34. D. J. RYLEY, *The present status of erosion studies in the wet steam turbine*, Prace Instytutu Maszyn Przepływowych, 42–44, 241–53, 1969.
35. D. J. RYLEY and J. SMALL, *Re-entrainment of deposited liquid from simulated steam turbine fixed blades*, Proceedings of the Conference on Heat and Fluid Flow in Steam and Gas Turbine Plant, Warwick 1973.
36. W. S. SARIC and B. W. MARSHALL, *An experimental investigation of the stability of a thin liquid layer adjacent to a supersonic stream*, AIAA-J., **9**, 8, 1546–53, 1971.
37. J. R. SCHUSTER, *Mass loss from thin liquid-surface films exposed to re-entry heating and shear*, J. Spacecraft, **9**, 4, 271–76, 1972.
38. A. SHERMAN and J. SCHETZ, *Breakup of liquid sheets and jets in a supersonic gas stream*, AIAA-J., **9**, 4, 666–73, 1971.
39. W. H. SHUTTS, W. H. HARTWIG and J. E. WEILER, *Final report on turbulent boundary-layer and skin-friction measurements on a smooth, thermally insulated flat plate at supersonic speeds*, Defense Res. Lab., Univ. of Texas, Rep. DRL-364, CM-823, 1955.
40. S. C. SOMMER and B. J. SHORT, *Free flight measurements of turbulent boundary-layer skin friction in the presence of severe aerodynamic heating at Mach numbers from 2.8 to 7.0*, NACA TN 3391, 1955.
41. C. O. WHITE and R. M. GRABOW, *Cross-hatch surface patterns. Comparison of experiment with theory*, AIAA-J., **11**, 9, 1316–1322, 1973.
42. M. WICKS, *Liquid film structure and drop size distribution in two-phase flow*, Diss. Univ. of Houston, 534, 1967.
43. R. E. WILSON, *Aerodynamic interference of Pitot-tubes in a turbulent boundary layer at supersonic speed*, AIAA-J., **11**, 10, 1420-21, 1973.
44. D. E. WURZ, *Flow behaviour of thin water films under the effect of a cocurrent air flow of moderate to high subsonic velocities; effect of the film on the air flow*, Proceedings of the third International Conference on Rain Erosion and Associated Phenomena. England, Evetham Hall, 11–13 August 1970, Vol. 2, 727–750. Published by A. A. Fyall and R. B. King, Royal Aircraft Establishment, England.
45. D. E. WURZ, *Experimentelle Untersuchung des Strömungsverhaltens dünner Wasserfilme und deren Rückwirkung auf einen gleichgerichteten Luftstrom mässiger bis hoher Unterschallgeschwindigkeit*, Diss. Universität Karlsruhe 1971.
46. D. E. WURZ, *Experimental investigation into flow behaviour of thin water films and their effect on a cocurrent air flow of moderate supersonic velocities*, Conference on Rain Erosion, Merseburg 1974.
47. G. L. BORDNER and A. M. NAYFEH, *Nonlinear stability of a liquid film adjacent to a viscous, supersonic stream*, Rept. E-74-11, April, 1974, Virginia Polytechnic Inst. and State Univ., Blacksbury, Va.
48. G. R. INGER and E. P. WILLIAMS, *Subsonic and supersonic boundary layer flow past a wavy wall*, AIAA-J, 10, 5, 636–642, 1972.
49. H. U. MEIER, *Experimentelle und theoretische Untersuchung von turbulenten Grenzschichten bei Überschallströmung*, Mitteilungen aus dem Max-Planck-Institut für Strömungsforschung und der AVA, Göttingen 1970.

INSTITUT FÜR THERMISCHE STRÖMUNGSMASCHINEN
UNIVERSITÄT KARLSRUHE.

http://rcin.org.pl